IJIE

INTERNATIONAL JOURNAL OF INTEGRATED ENGINEERING
ISSN: 2229-838X e-ISSN: 2600-7916

Vol. 18 No. 2 (2026) 307-319
https://publisher.uthm.edu.my/ojs/index.php/ijie

Tensile Strength, Microstructure, and Fractography Analysis of FDM 3D Printed Parts Using Self-Made PLA-Brass Filaments

Mahros Darsin[1]*, Indra Cahyo Kuncoro[1], Nasrul Ilminnafik[1], R. Koekoeh Koentjoro Wibowo[1], Agus Triono[1], Mohd Sabri Hussin[2]

[1] *Department of Mechanical Engineering, Faculty of Engineering, University of Jember, Jember, 68121, INDONESIA*
[2] *Department of Mechanical Engineering, Faculty of Engineering & Technology, University Malaysia Perlis, Perlis, 02600, MALAYSIA*

*Corresponding Author: mahros.teknik@unej.ac.id
DOI: https://doi.org/10.30880/ijie.2026.18.02.024

Article Info

Received: 15 November 2025
Accepted: 24 April 2026
Available online: 16 June 2026

Keywords

3D printing, PLA-brass filaments, tensile strength

Abstract

Manufacturing technology development has experienced various innovations, including 3D printing. The progress of 3D printing has been adopted in various fields. This study explores the innovations in manufacturing technology, particularly the advancement of 3D printing and its application in producing metal alloy filaments. The focus is on creating an innovation using PLA-brass filament, with extruder temperature, layer height, and print speed as control parameters. The objective is to distinguish the ideal combination of these 3D printing parameters to realise the greatest ductile quality. Through the Taguchi method application, the aim is to enhance product quality while reducing fabrication costs. An L4(2)3 orthogonal matrix is employed, leading to four experimental combinations replicated three times, amounting to twelve experiments overall. The data obtained from tensile testing is then analysed using Analysis of Variance (ANOVA) to determine which parameters significantly impact the test results. This study concludes that the optimal tensile strength is achieved with an extruder temperature of 230°C, a print speed of 20 mm/s, and a layer height of 0.2 mm. The analysis also reveals that extruder temperature contributes 38.81% to the tensile strength results, followed by layer height at 17.5%, and print speed at 15.26%

1. Introduction

The development of manufacturing technology today has experienced various innovations that increase the quality to compete in the market. One of the innovations that is on the rise today is 3D printing. 3D printing has been adopted globally by the medical, automobile, aerospace, military, food industry, and other related sectors due to the easy and customizable fabrication of prototypes, functional models, and conceptual models [1]. 3D printing technology, called Additive manufacturing, makes three-dimensional objects by arranging thin layers sequentially until an object is formed using computer-aided manufacturing (CAM). After a 3D-printed filament is heated to be extruded through a nozzle, it is often relatively rapidly cooled [2]. This process makes it possible to produce components by combining or melting solid-state [3].

3D printing technology can provide various advantages in the manufacturing process, not only being considered faster, but also can make various shapes or complicated dimensions accurately. It can be seen in various manufacturing fields that utilize 3D printing technology to make 3D objects because of its potential and advantages. The advantage of 3D printing is that it allows ideas to develop faster. They can print concepts and designs on the same day to reduce the development process that may take months to days, helping companies be one step ahead of others. 3D printing technology is revolutionizing the manufacturing industry with an innovative and disruptive approach to product manufacturing [4]. However, in spite of the numerous advantages of 3D printing, the need for quality products made by 3D printing has limited the use of products in the industry [5].

There are multiple 3D printing methods, with fused deposition modelling (FDM) being particularly widespread due to its affordability, low power consumption, and ease of trialling complex designs [6]. In FDM, a thermoplastic filament is fed into a heated nozzle where it melts and is deposited in successive lines and layers to recreate the intended three-dimensional geometry. The mechanical performance of FDM-printed parts is highly dependent on numerous processing parameters, such as nozzle and build-plate temperatures, printing speed and orientation, layer height, raster angle, and infill pattern [7]. Among these variables, print orientation, raster direction, infill strategy, and layer thickness play especially critical roles in defining the final polymer properties of the printed components [8]. The most commonly employed filaments are Polylactic Acid (PLA) and Acrylonitrile Butadiene Styrene (ABS). PLA, a biodegradable thermoplastic derived from lactic acid, has found extensive application in areas such as cardiovascular implants, dental scaffolds, drug delivery systems, orthopaedic devices, and food packaging [9].

Recent advances in 3D printing have driven continuous innovation in thermoplastic filament offerings, particularly in their base formulations, mechanical performance, and dimensional specifications. A notable trend is the development of hybrid filaments that combine thermoplastics with metal alloys. Likewise, metal–polymer composites—created by blending metals or thermoplastics in specific proportions—have garnered significant attention in recent studies [10]. To further enhance the performance of PLA-based prints, various fillers have been incorporated into PLA composites [11]. In this work, tensile tests were performed on in-house–produced PLA–brass filaments, with extruder temperature, printing speed, and layer height defined as the three controlled variables.

2. Materials and Method

2.1 Tools and Materials

This study focuses on the effect of 3D printing parameters on the tensile strength value. The filament used is a thermoplastic alloy filament, specifically PLA-brass, procured from the University of Jember lab, Indonesia. The brass powder used has a size of 100 mesh, while the PLA is in granule form with a diameter of 3-4 mm, which can be purchased from the market and extruded into filament form. The composition of this filament is 60% PLA and 40% brass.

To produce the self-made PLA-brass filaments, the PLA granules and brass powder are first weighed according to the desired composition (60% PLA and 40% brass). The materials are then thoroughly mixed to ensure a uniform distribution of brass particles within the PLA matrix. This mixture is fed into a filament extruder, which heats the mixture to a temperature range of 190°C - 195°C, melting the PLA and allowing it to encapsulate the brass particles. The molten mixture is then forced through a die to form a continuous filament with a diameter of 1.75 mm. As the filament exits the extruder, it passes through a cooling system to solidify. The cooling system typically consists of a water bath or air cooling setup to ensure the filament maintains its shape and diameter. Once solidified, the filament is wound onto spools for storage and later use in 3D printing.

The PLA–brass composite filament was fabricated on an Ender 3 V2 3D printer using the FDM approach. During printing, the material is heated and extruded through a 0.6 mm circular nozzle, depositing successive layers to build the part. Key parameters—nozzle temperature, bed temperature, and print speed—were systematically tuned to optimize both print fidelity and mechanical performance. A view of the custom filament alongside the printer setup is provided in Fig. 1.

(a) (b)

Fig. 1 *Filament PLA-Brass and 3D printer Ender 3 V2*

2.2 Taguchi Method

The Taguchi system is a widely acknowledged and effective methodology that offers a systematic and practical approach to optimizing designs. Its significance becomes particularly evident in the context of rapid prototyping, where the production costs of prototypes remain high. By employing a Taguchi matrix, which is an orthogonal array, the system facilitates the identification of a set of experimental runs [12]. These runs allow engineers and designers to efficiently explore and analyze the various factors that impact the design's performance and quality.

Rapid prototyping is a crucial phase in the product development process, where physical prototypes are quickly produced to evaluate the design's functionality and suitability. However, conducting multiple experiments to assess different design parameters can be costly and time-consuming. Here, the Taguchi system's value shines through as it optimizes the experimental process, reducing the number of required tests while maintaining the accuracy and relevance of the results. This cost and time-saving feature is especially beneficial during the initial stages of development when iterating and refining the design. At the heart of the Taguchi system lies the Taguchi matrix, an orthogonal array that determines the most effective combination of experimental runs. This matrix is designed to ensure that essential design factors and their various levels are adequately explored, providing valuable insights into their influence on the overall design performance. By employing the Taguchi matrix, engineers can make informed decisions about the design parameters that meaningfully influence the final quality of products and efficiency.

In conjunction with the Taguchi matrix, the Design Matrix plays a critical role in organizing and planning the experimental runs. It is a comprehensive table that captures all possible combinations of levels for the different factors involved in the design process [13]. This systematic representation of design factors ensures that nothing is overlooked and helps engineers consider all relevant aspects during the optimization process.

2.3 Response Parameters

The researcher determines the parameters used in this study and acts as the object of research. These parameters also directly affect the test results. The control parameters are extruder temperature, print speed, and layer height. Variations in values at each parameter level were obtained from previous experiments and research in previous journals. Parameter variations in this research can be seen in Table 1.

Table 1 *Factor value of each parameter*

Factor	Level 1	Level 2
Nozzle Temperature (°C)	230	240
Print Speed (mm/s)	20	30
Layer Height (mm)	0.2	0.3

2.4 Experimental Design

At this stage, it is carried out through various stages. From the stage of making tensile test specimen design, the stage of making 3D models, to the testing stage. The FDM process includes applications starting from prototypes to functional parts. Creation of the CAD model, conversion of the CAD model into the STL (stereo-lithography) format, slicing of the STL format into thin layers, construction of the part in a layer-by-layer fashion, and cleaning and finishing are the five simple steps utilized in the FDM process to manufacture a component [14] —the manufacturing of specimens made based on ASTM type V. The specimens for tensile testing were configured with the shape and key geometric dimensions shown in Fig. 2.

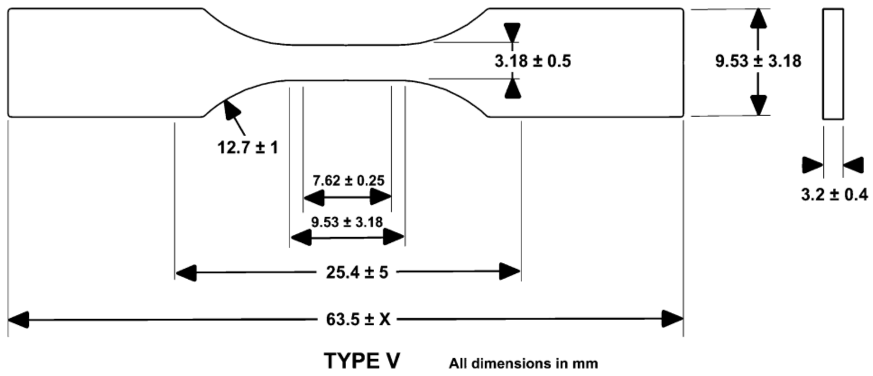

Fig. 2 *ASTM D638 tensile test specimen type V [15]*

The specimen design model will be made using CAD software and continued with the slicing process so that a G-code is obtained that will be used to manufacture using consumer-grade 3D printers [16]. The Simplify3D slicer was employed to configure the various parameters of the 3D printing process [17]. There were 12 tensile test specimens, of which there were four kinds of parameter combinations, and each combination was replicated three times, so that there were 12 pairs according to the Taguchi method of orthogonal matrix $L_4(2^3)$ used in this study. This method aims to reduce production costs and resources spent to a minimum with production processes and results as optimally as possible according to objectives, without being influenced by external factors. Besides, the gage length in ASTM D638 type V was specified as 25.4 mm, which is the proper space for measurement [18].

Stress is defined as the load or force per unit area of cross-section, or can be formulated as follows:

$$\sigma = \frac{p}{A} \tag{1}$$

Information:

σ = Tensile strength (kg/mm^2)

p = Force (kg)

A = Cross-sectional area (mm^2)

This study used the S/N ratio of Larger is Better. The higher the tensile test results obtained, the more influential the parameters used. Following the expectations of testing, namely, to obtain test results with the highest tensile strength. The calculation table of the S/N ratio with the Larger is Better criterion can be seen in the following equation:

$$\text{S/N Ratio Larger is Better} = -10log\left(\frac{1}{n}\sum_{i=n}^{n}\frac{1}{y_i^2}\right) \tag{2}$$

2.5 Universal Testing Machine

The tensile samples were tested on a UTM configured according to ASTM D638 Type V at a constant crosshead speed of 10 mm/min. Mechanical metrics—yield strength, peak load, ultimate tensile strength, elongation at break, and the stress–strain behavior—were recorded during these tests. The modulus of toughness was determined from the stress–strain curve using the prescribed equation [19]. Fig. 3 depicts the filament together with the testing setup.

Fig. 3 *Real-time UTM testing setup as per ASTM D638 type V*

3. Results and Discussions

3.1 Taguchi Analysis

Sample specimens were fabricated in accordance with the dimensional requirements and tolerance limits specified by ASTM D638 Type V of the American Society for Testing and Materials. The reason for using type V is that type V is an overall reduced specimen from type I, requiring less material in its manufacture. In addition, type V is also considered to produce a good level of accuracy, as in type I. After the specimen is considered excellent and suitable for testing, a tensile test is performed using a universal testing machine with type HT-2402. After tensile testing of the test specimen, a fracture occurred in the Gauge Length, which was 25.4 mm long, in the middle of the specimen. The specimens before and after the tensile test results can be seen in Fig. 4.

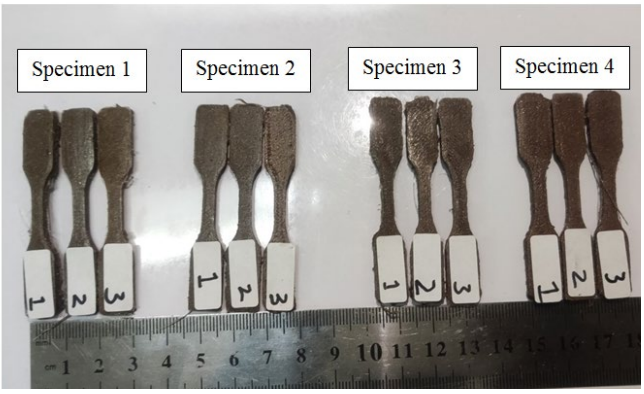

(a)

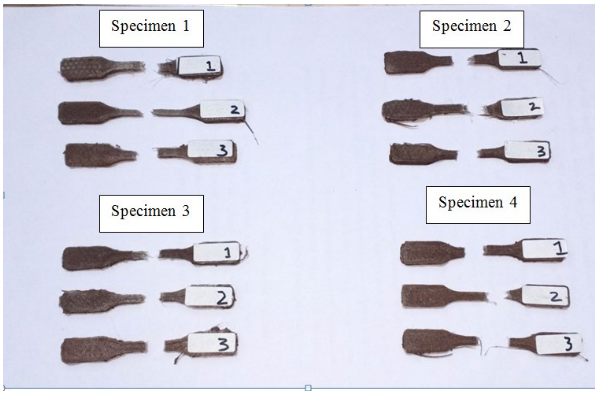

(b)

Fig. 4 *Specimen (a) Before; (b) After the tensile test result*

Analysis of the test results revealed that a 230 °C extruder temperature, 20 mm/s print speed, and 0.2 mm layer height yielded the highest tensile strength of 11.87 N/mm^2, whereas a 240 °C extruder temperature, 20 mm/s print speed, and 0.3 mm layer height produced the lowest tensile strength of 5.80 N/mm^2. Specimen tensile test data are summarized in Table 2.

Table 2 *Data table of tensile test results*

Experiment	Control Parameters			Tensile Strength Value (N/mm^2).			Average	S/N Ratio
				Replication				
	Extruder Temperature (°C)	Print Speed (mm/s)	Layer Height (mm)	1	2	3		
1	230	20	0.2	10.70	10.50	11.87	11.02	20.81
2	230	30	0.3	8.23	6.44	9.07	7.91	17.69
3	240	20	0.3	5.80	6.88	8.70	7.13	16.71
4	240	30	0.2	8.57	6.20	6.29	7.02	16.65

3.2 S/N Ratio Analysis

Within this design framework, the Taguchi approach is used to identify the most effective parameter settings. For each factor, the ideal level is determined by calculating its signal-to-noise (S/N) ratio across all levels. The "Larger Is Better" S/N ratio for selecting the optimal setting (parameter 1 = extruder temperature) is then computed as follows:

$$\bar{A}_1 = \frac{20.81 + 17{,}69}{2}$$

$$\bar{A}_1 = 19.25$$

A consistent procedure was applied to compute the "Larger Is Better" S/N ratio for experiments two, three, and four. The resulting optimal factor–level settings derived from this analysis are listed in Table 3.

Table 3 *S/N ratio: Larger is better*

Level	Extruder Temperature	Print Speed	Layer Height
1	19.25	18.76	18.73
2	16.28	17.17	17.20
Delta	2.57	1.59	1.53
Rank	1	2	3

Details of the S/N ratio are presented as a graph plot in Fig. 5.

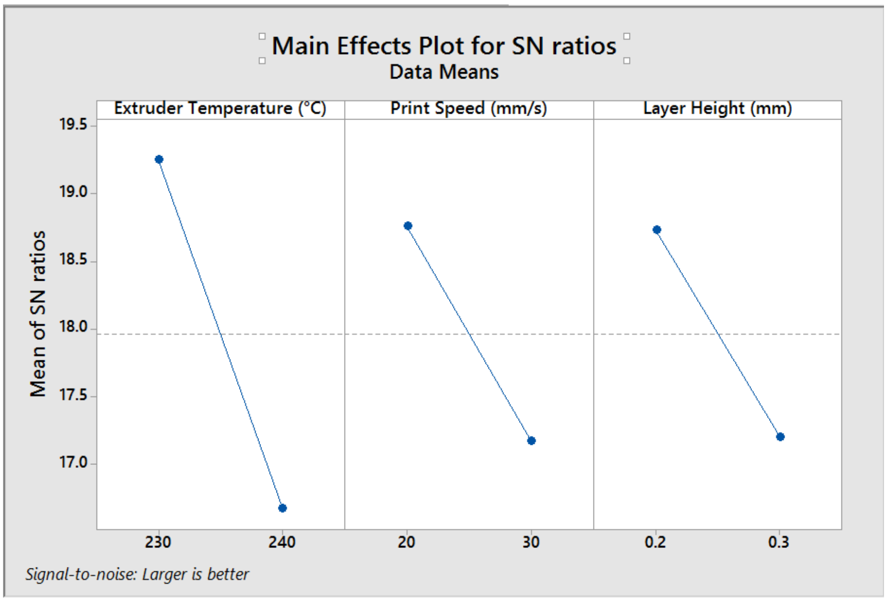

Fig. 5 *Plot S/N ratio: Larger is better*

From the graph in Fig. 4, the optimal parameters of the test can be seen in Table 4.

Table 4 *Optimal parameter*

Control Parameter	Level	Value
Nozzle Temperature	1	230°C
Print Speed	1	20 mm/s
Layer Height	1	0.2 mm

3.3 Tensile Properties

Fig. 6 shows the stress–strain curves for the PLA-Brass specimens according to the parameters. The curve is compiled for all experiments that have been carried out. In the PLA-Brass filaments, it is observed that the stress increases linearly. After the stress peaked, it was nearly constant with increasing strain, indicating that adding the brass powder to the PLA can change the PLA matrix from brittle to ductile. It can be seen that experiment 1, replication 3, has a graph with the broadest range compared to other experiments. Experiment 1, replication 3, likewise showed the highest tensile strength at 11.87 N/mm^2 and yield strength at 8.12 N/mm^2. Besides, the minimum tensile strength and yield strength recorded were also found in experiment 3 replication 1, with values of 5.80 N/mm^2 and 4.13 N/mm^2.

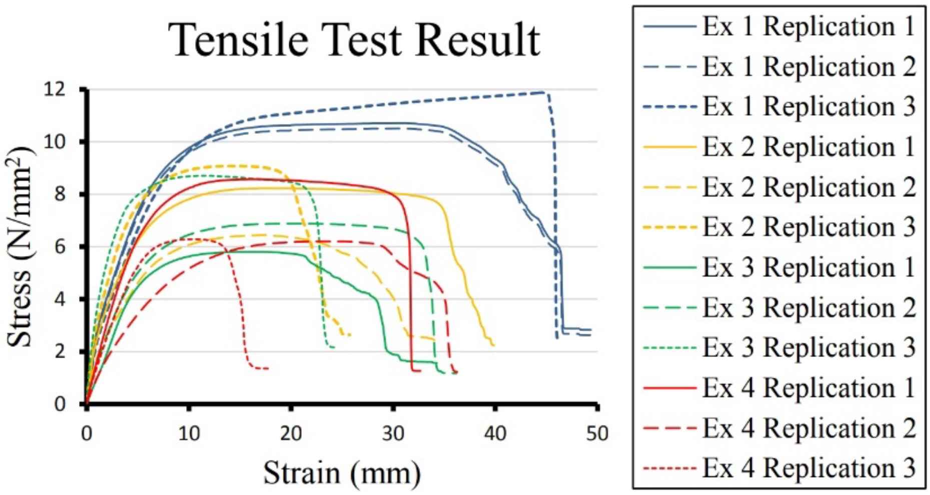

Fig. 6 *Tensile stress-strain profiles of PLA-Brass specimens*

Figure 6 illustrates the stress–strain response of PLA–Brass samples under the tested parameter settings. The curve is compiled for all experiments that have been carried out. In the PLA-Brass filaments, it is observed that the stress increases linearly. After the stress peaked, it was nearly constant with increasing strain, indicating that adding the brass powder to the PLA can change the PLA matrix from brittle to ductile. It can be seen that experiment 1, replication 3, has a graph with the broadest range compared to other experiments. The maximum tensile strength and yield strength recorded were also found in experiment 1 replication 3, with values of 11.87 N/mm^2 and 8.12 N/mm^2. Besides, the minimum tensile strength and yield strength recorded were also found in experiment 3 replication 1, with values of 5.80 N/mm^2 and 4.13 N/mm^2.

Comparison with Other PLA Filaments. For a complete assessment, the tensile strength values of the PLA-Brass filaments were compared with those of standard PLA filaments and several other composite PLA filaments. Standard PLA filaments typically exhibit tensile strength values ranging from 50 to 70 MPa [20] (Composite PLA filaments with various fillers show a wide range of tensile strengths depending on the filler type and concentration. For instance, PLA-carbon fiber composites can achieve tensile strengths up to 90 MPa [21], whereas PLA-wood composites generally have lower tensile strengths around 30 MPa [22].

The comparison highlights that while the PLA-Brass filaments produced in this study have lower tensile strength values compared to some other composite PLA filaments, they offer unique properties such as enhanced ductility and potential applications where a balance between strength and flexibility is required.

3.4 ANOVA

Analysis of Variance (ANOVA) is employed to derive statistical insights from experimental data. This technique assesses the extent to which each factor influences the measured responses. By quantifying these contributions, ANOVA guides the selection of parameter settings for developing predictive models.

ANOVA is performed using the mean values from the data table. Since Taguchi's experimental layout involves multiple factors at several levels, a two-way analysis of variance is applied. This process calculates the degrees of freedom, sums of squares, mean squares, and F-values. The resulting ANOVA data, which reveal each control factor's effect on tensile strength, are shown in Table 5.

Table 5 *Tensile strength ANOVA*

Control Parameter	DoF	SS	MS	F value	P	Contribution
Extruder Temperature	1	17.21	17.21	10.92	Significant	38.81 %
Print Speed	1	7.76	7.76	4.92	Significant	15.26 %
Layer Height	1	6.77	6.77	4.29	Significant	17.50 %
Error	8	12.61	1.58	1.00	Significant	28.43 %
Total	11	44.34	33.31	21.14		100.00 %

4. Effect of Printing Parameters on Tensile Strength

4.1 Effect of Extruder Temperature

The extruder temperature parameter is the most significant factor in determining the tensile strength value, with a contribution rate of 38.81%. The extruder temperature directly affects the bonding process layer by layer. At 240°C, the filament melts into a too-liquid state, causing the filament to flow too freely and resulting in suboptimal specimen filling. This observation mirrors the conclusions of Darsin et al. (2022), who reported that nozzle temperature during 3D printing has a significant impact on the tensile strength and mechanical characteristics of materials [23]. Nozzle temperature also plays a vital role in adhesion between layers during printing, as higher temperatures can improve interlayer bonding but may also lead to excessive flow and poor structural integrity [24].

4.2 Effect of Layer Height

The height of the layers is the second most significant factor, accounting for 17. 5% of this study's total influence. The layer height determines how thick each layer is in the printed specimen. Thinner layers lead to more layers making up the molded product, which increases the tensile strength value. Thinner layer heights also reduce porosity due to the tighter distance between layers. This statement is supported by previous research, emphasizing that the highest tensile strength value is attained at the lowest thickness [25]. The lower the distance between the layers, the more layers are created, resulting in a high bonding area between layers. Lower layer heights improve adhesion between layers, leading to better mechanical properties [26].

Layer height—often called layer thickness—substantially influences the printed part's surface quality, mechanical strength, and printing speed. Smaller layer heights result in finer details and smoother surfaces because the layers are thinner and less noticeable. This is particularly important for prints requiring high precision and aesthetic quality, such as detailed models. Thicker layers can sometimes lead to weaker bonds between layers, resulting in a less robust print. Conversely, thinner layers can improve the inter-layer adhesion, leading to stronger prints. However, this also depends on the material used and the specific printing conditions [27].

Different materials have different optimal layer heights. For example, PLA is versatile and can be printed at a wide range of layer heights, while ABS is better suited for thicker layers. Nylon requires careful cooling and may perform better with specific layer heights [28].

4.3 Effect of Print Speed

The print speed parameter has the lowest contribution, at 15.26%. At high-speed settings, the melted filament cannot adhere to the bed thoroughly. The nozzle's movement speed makes the filament extrusion process not maximally efficient. It remains attached to the nozzle, causing filling failure and structures that do not follow the design. The print speed parameter must be set more slowly so that the filament extrusion process takes place properly and can fill the printed specimen thoroughly to produce prints with a denser and more robust structure.

This finding aligns with Maguluri et al. (2023), who identified print speed as a key factor influencing the tensile behavior of 3D-printed materials [29]. At lower speeds, the molten filament flows and deposits more uniformly due to its enhanced fluidity. Slower extrusion also elevates the temperature at the interface between successive layers, strengthening interlayer adhesion and boosting tensile strength. Similarly, Dou et al. (2020) showed that continuous 3D-printed composites achieve superior tensile mechanical properties when printed at reduced speeds [30].

Taking into account the combined effects of all three variables on tensile strength measurements, it can be concluded that the study's results do not apply to 3D-printed products due to their low tensile performance. The highest average tensile strength for PLA–Brass reached just 11.02 N/mm², which remains insufficient for manufacturing applications.

5. Microstructure

The subsequent analysis process in this study is microstructure analysis. Analysis of the microstructure is performed to identify the makeup of the sample and how this structure affects its mechanical characteristics. Microstructure analysis in this study is through two methods, namely fractographic analysis and microanalysis.

5.1 Fractographic Analysis

Fractographic examination of the fractured regions was conducted with a digital microscope to characterize failure modes in the gauge section of the 3D-printed polymers [25]. This analysis reveals the various fracture patterns that influence the specimens' mechanical behavior. It focused on specimen one, third replication (highest tensile strength of 11.87 N/mm²), and specimen four, second replication (tensile strength of 6.20 N/mm²), allowing a direct comparison between samples with the greatest and lowest strength values. The resulting fractographic images are presented in Fig. 7.

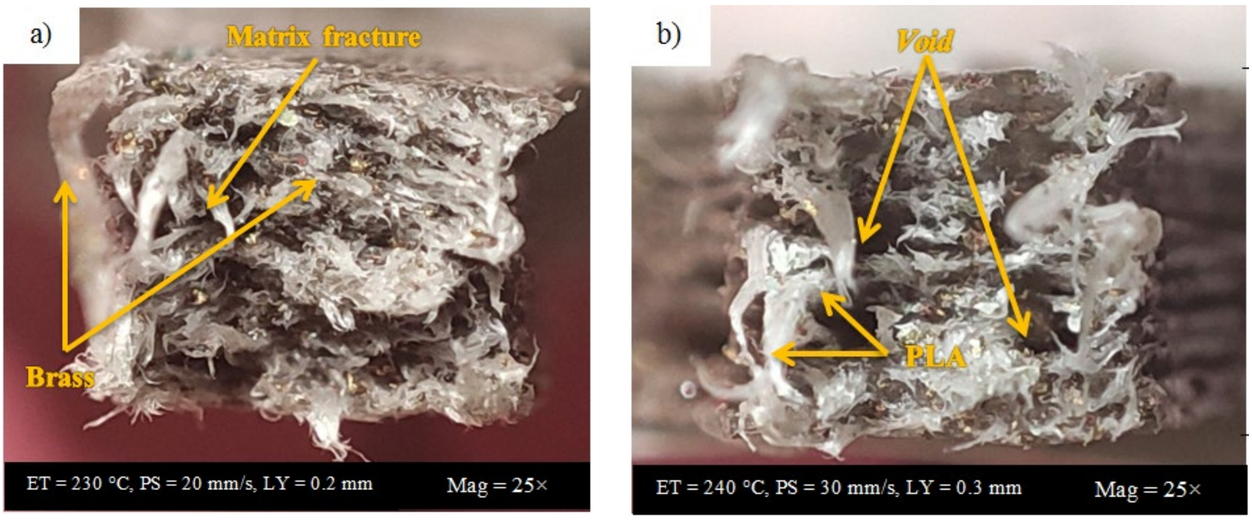

(a) **(b)**

Fig. 7 *Specimen fracture with average tensile strength (a) Highest; (b) Lowest*

Fig. 7 shows the fractured part of the specimen after tensile testing. Fig. 7 shows a dense arrangement of layers and almost no voids. The white part of the fault indicates PLA's ability to deform. The brass particles in Fig. 7, a fractured part, are also more than in Fig. 7 b. Fig. 7 b shows that there are several voids in the layer. This void arises due to indiscretion in the printing process. More voids appearing also further reduce the specimen's tensile strength value.

5.2 Micro Analysis

The micro-analysis process is carried out to determine the constituent structure of specimens made from brass PLA filaments. The microstructure of brass PLA filaments before and after the printing process can be seen in Fig. 8.

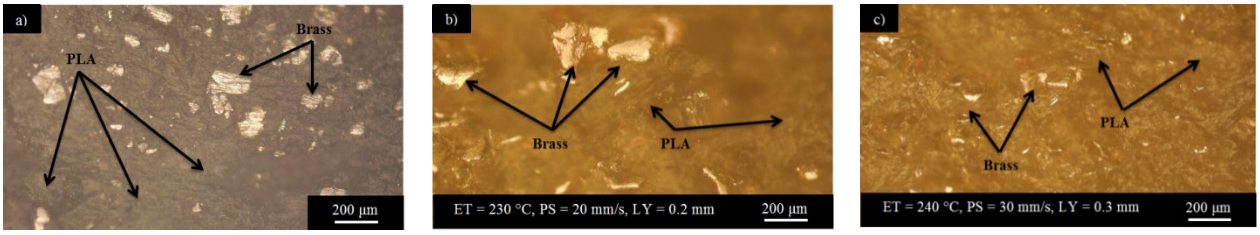

(a) **(b)** **(c)**

Fig. 8 *Comparison of the microstructure between filaments and specimens: (a) Filament; specimen with the (b) Highest; and (c) Lowest tensile strength*

The results of the microstructure test on the brass PLA filament show that the distribution of the brass area is concentrated in part of the area, and PLA fills part of the area. The analysis process is carried out using an optical microscope. Furthermore, microstructure analysis was carried out on specimen one, triple replication, which showed the highest tensile strength value of 11.87 N/mm^2, with specimen four replication two with a tensile strength value of 6.20 N/mm^2. The results of microstructure testing can be seen in Fig. 8 b and c. The microstructure analysis results in Fig. 8 show that the 3D printed specimens of brass PLA filaments in figures b and c have only slight differences. The white part in the image shows brass particles, while the yellow part shows the PLA content. It follows the opinion of previous studies[26] that the bright white spot part is a metal particle. In the results of specimen analysis, it can be seen that the distribution of the brass material area is less even. In specimens with higher tensile strength values, brass area distribution is more even than in specimens with the lowest tensile strength values.

The results of the microstructure test on the brass PLA filament show that the distribution of the brass area is concentrated in part of the area, and PLA fills part of the area. The analysis process is carried out using an optical microscope. Furthermore, microstructure analysis was carried out on specimen one, triple replication, which showed the highest tensile strength value of 11.87 N/mm^2, with specimen four replication two with a tensile strength value of 6.20 N/mm^2. The results of microstructure testing can be seen in Fig. 8 b and c. The microstructure analysis results in Fig. 8 show that the 3D printed specimens of brass PLA filaments in figures b and c have only slight differences. The white part in the image shows brass particles, while the yellow part shows the PLA content. It follows the opinion of previous studies [31] that the bright white spot part is a metal particle. In the results of specimen analysis, it can be seen that the distribution of the brass material area is less even. In specimens with higher tensile strength values, brass area distribution is more even than in specimens with the lowest tensile strength values.

To provide a comprehensive analysis, the microstructure of the brass PLA filaments was compared with that of other composite PLA filaments. Research has demonstrated that the mechanical performance of composite filaments is strongly governed by both the size and spatial distribution of their filler particles. For instance, PLA-carbon fiber composites exhibit a more uniform distribution of carbon fibers, leading to enhanced tensile strength and stiffness [32]. In contrast, PLA-wood composites often show a less uniform distribution of wood particles, resulting in lower tensile strength [22]. The comparison highlights that while the brass PLA filaments produced in this study have a less uniform distribution of brass particles, they offer unique properties such as enhanced ductility and potential applications where a balance between strength and flexibility is required.

6. Conclusion

This study investigates the effect of 3D printing parameters on the tensile strength of PLA–brass composites. The results indicate that extruder temperature is the most influential factor, accounting for 38.81% of the observed variation in tensile strength. By carefully selecting the appropriate extruder temperature, manufacturers can significantly enhance layer bonding and improve tensile strength. Layer height also plays a substantial role, contributing 17.5% to tensile strength variations. An optimal layer height increases the number of constituent layers, enhancing bonding and producing stronger specimens. While print speed has the smallest effect, contributing 15.26%, it remains a crucial factor. Optimizing the print speed ensures effective filament extrusion, resulting in denser and more robust prints, ultimately improving tensile strength.

The optimal combination of parameters—an extruder temperature of 230°C, a print speed of 20 mm/s, and a layer height of 0.2 mm—produces PLA-brass products with superior tensile strength properties. These findings emphasize the importance of carefully controlling 3D printing parameters to enhance product quality and mechanical performance.

Producers and investigators of PLA-brass filament items can use this knowledge to improve products for a variety of uses, including rapid prototyping as well as the practical applications of such components in automotive, aerospace, or consumer products. As the adoption of 3D printing continues to grow, this research provides valuable knowledge to drive advancements in additive manufacturing technologies and material engineering.

Acknowledgement

The authors would like to acknowledge the Laboratory of Manufacturing Processes at the Faculty of Engineering, University of Jember, for facilitating this research.

Conflict of Interest

The authors declare that there is no conflict of interest regarding the publication of the paper.

Author Contribution

The authors confirm contribution to the paper as follows: ***study conception and design:*** *Mahros Darsin, Indra C. Kuncoro, Agus Triono;* ***data collection:*** *Indra C. Kuncoro, R. Koekoeh K. Wibowo;* ***analysis and interpretation of results:*** *Mahros Darsin, Nasrul Ilminnafik;* ***draft manuscript preparation:*** *Indra C. Kuncoro, Agus Triono;* ***final paper checking:*** *Mahros Darsin, Mohd Sabri Hussin. All authors reviewed the results and approved the final version of the manuscript.*

References

[1] Vardhan, H., Kumar, R., & Chohan, J. S. (2020). Investigation of tensile properties of sprayed aluminium based PLA composites fabricated by FDM technology. *Materials Today: Proceedings*, 33, 1599-1604. https://doi.org/10.1016/j.matpr.2020.05.335

[2] Zisopol, D. G., Portoaca, A. I., Nae, I., & Ramadan, I. (2022). A comparative analysis of the mechanical properties of annealed PLA. Engineering, *Technology & Applied Science Research*, 12(4), 8978-8981. https://doi.org/10.48084/etasr.5123

[3] Pandey, R., & Ramani, H. B. (2021). A study of metallurgical and processing approach of additive layer manufacturing processes for metal tool components production. *Materials Today: Proceedings*, 47, 6642-6646. https://doi.org/10.1016/j.matpr.2021.05.103

[4] Arpan, M. F. Z. I. B. M., & Hoong, L. J. (2019, August). Effect of printing temperature on mechanical properties of copper metal polylactide acid. In *AIP Conference Proceedings* (Vol. 2137, No. 1, p. 040003). AIP Publishing LLC. https://doi.org/10.1063/1.5121001

[5] Seol, K. S., Zhao, P., Shin, B. C., & Zhang, S. U. (2018). Infill print parameters for mechanical properties of 3D printed PLA parts. *Journal of the Korean Society of Manufacturing Process Engineers*, 17(4), 9-16. https://doi.org/10.14775/ksmpe.2018.17.4.009

[6] W. Ahmed, S. Siraj, and A. H. Al-Marzouqi, "3D Printing PLA Waste to Produce Ceramic Based Particulate Reinforced Composite Using Abundant Silica-Sand: Mechanical Properties Characterization," *Polymers (Basel)*, vol. 12, no. 11, p. 2579, Nov. 2020, https://doi.org/10.3390/polym12112579

[7] Z. Liu, Q. Lei, and S. Xing, "Mechanical characteristics of wood, ceramic, metal and carbon fiber-based PLA composites fabricated by FDM," *Journal of Materials Research and Technology*, vol. 8, no. 5, pp. 3741–3751, Sep. 2019, https://doi.org/10.1016/j.jmrt.2019.06.034

[8] M. M. Hanon, Y. Alshammas, and L. Zsidai, "Effect of print orientation and bronze existence on tribological and mechanical properties of 3D-printed bronze/PLA composite," *The International Journal of Advanced Manufacturing Technology*, vol. 108, no. 1–2, pp. 553–570, May 2020,

https://doi.org/10.1007/s00170-020-05391-x.

[9] H. Chokshi, D. B. Shah, K. M. Patel, and S. J. Joshi, "Experimental investigations of process parameters on mechanical properties for PLA during processing in FDM," *Advances in Materials and Processing Technologies*, vol. 8, no. sup2, pp. 696–709, Sep. 2022, https://doi.org/10.1080/2374068X.2021.1946756

[10] Ü. Çevik and M. Kam, "A Review Study on Mechanical Properties of Obtained Products by FDM Method and Metal/Polymer Composite Filament Production," *J Nanomater*, vol. 2020, pp. 1–9, Nov. 2020, https://doi.org/10.1155/2020/6187149

[11] M. C. Vu, T. Jeong, J. Kim, W. K. Choi, D. H. Kim, and S. Kim, "3D printing of copper particles and poly(methyl methacrylate) beads containing poly(lactic acid) composites for enhancing thermomechanical properties," *J Appl Polym Sci*, vol. 138, no. 5, Feb. 2021, https://doi.org/10.1002/app.49776

[12] Babagowda, R. S. Kadadevara Math, R. Goutham, and K. R. Srinivas Prasad, "Study of Effects on Mechanical Properties of PLA Filament which is blended with Recycled PLA Materials," *IOP Conf Ser Mater Sci Eng*, vol. 310, p. 012103, Feb. 2018, https://doi.org/10.1088/1757-899X/310/1/012103

[13] J. Xu, F. Xu, and G. Gao, "The Effect of 3D Printing Process Parameters on the Mechanical Properties of PLA Parts," *J Phys Conf Ser*, vol. 2133, no. 1, p. 012026, Nov. 2021, doi: 10.1088/1742-6596/2133/1/012026.

[14] T. Mengesha Medibew, "A Comprehensive Review on the Optimization of the Fused Deposition Modeling Process Parameter for Better Tensile Strength of PLA-Printed Parts," *Advances in Materials Science and Engineering*, vol. 2022, pp. 1–11, Aug. 2022, https://doi.org/10.1155/2022/5490831

[15] A. R. Torrado Perez, D. A. Roberson, and R. B. Wicker, "Fracture Surface Analysis of 3D-Printed Tensile Specimens of Novel ABS-Based Materials," *Journal of Failure Analysis and Prevention*, vol. 14, no. 3, pp. 343–353, Jun. 2014, https://doi.org/10.1007/s11668-014-9803-9

[16] D. Farbman and C. McCoy, "Materials Testing of 3D Printed ABS and PLA Samples to Guide Mechanical Design," in *Volume 2: Materials; Biomanufacturing; Properties, Applications and Systems; Sustainable Manufacturing*, American Society of Mechanical Engineers, Jun. 2016. doi: 10.1115/MSEC2016-8668.

[17] M. M. Hanon, R. Marczis, and L. Zsidai, "Influence of the 3D Printing Process Settings on Tensile Strength of PLA and Influence of the 3D Printing Process Settings on Tensile Strength of PLA and HT-PLA," *Periodica Polytechnica Mechanical Engineering Influence*, vol. 65, no. November, pp. 1–9, 2020, https://doi.org/10.3311/PPme.13683

[18] M. Aydin and Ö. Öz, "Application of Digital Image Correlation Technique to Tensile Test for Printed PLA Specimens," *International Journal of 3D Printing Technologies and Digital Industry*, vol. 2, no. 2, pp. 1–7, 2018.

[19] S. Kumar, R. Singh, and M. Singh, "Multi-material 3D printed PLA/PA6-TiO2 composite matrix: rheological, thermal, tensile, morphological and 4D capabilities," *Advances in Materials and Processing Technologies*, vol. 8, no. 2, pp. 2329–2348, Apr. 2022, https://doi.org/10.1080/2374068X.2021.1912527

[20] S. Farah, D. G. Anderson, and R. Langer, "Physical and mechanical properties of PLA, and their functions in widespread applications — A comprehensive review," *Adv Drug Deliv Rev*, vol. 107, pp. 367–392, Dec. 2016, https://doi.org/10.1016/j.addr.2016.06.012

[21] N. Maqsood and M. Rimašauskas, "Characterization of carbon fiber reinforced PLA composites manufactured by fused deposition modeling," *Composites Part C: Open Access*, vol. 4, p. 100112, Mar. 2021, https://doi.org/10.1016/j.jcomc.2021.100112

[22] V. U. Siddiqui, J. Yusuf, S. M. Sapuan, M. Z. Hasan, M. M. Mudah Bistari, and Z. G. Mohammadsalih, "Mechanical Properties and Flammability Analysis of Wood Fiber Filled Polylactic Acid (PLA) Composites Using Additive Manufacturing," *Journal of Natural Fibers*, vol. 21, no. 1, Dec. 2024, https://doi.org/10.1080/15440478.2024.2409868

[23] M. Darsin, R. R. Mauludy, I. Hardiatama, B. A. Fachri, M. E. Ramadhan, and D. Parningotan, "Analysis of the effect 3D printing parameters on tensile strength using Copper-PLA filament," *SINERGI*, vol. 26, no. 1, p. 99, Feb. 2022, https://doi.org/10.22441/sinergi.2022.1.013

[24] P. Gkertzos, A. Kotzakolios, G. Mantzouranis, and V. Kostopoulos, "Nozzle temperature calibration in 3D printing," *International Journal on Interactive Design and Manufacturing (IJIDeM)*, vol. 18, no. 2, pp. 879–899, Mar. 2024, https://doi.org/10.1007/s12008-023-01681-2

[25] J. M. Chacón, M. A. Caminero, E. García-Plaza, and P. J. Núñez, "Additive manufacturing of PLA structures using fused deposition modelling: Effect of process parameters on mechanical properties and their optimal selection," *Mater Des*, vol. 124, pp. 143–157, Jun. 2017, https://doi.org/10.1016/J.MATDES.2017.03.065

[26] C. Drugă, I. Șerban, B. Braun, and A. Tulică, “Analysis of the Influence of the Layer Height on the Strength of 3D Printed Structures,” in *11th International Conference on Information Science and Information Literacy*, Sciendo, 2021, pp. 177–181. https://doi.org/10.2478/9788395815065-019

[27] 3dprinterly.com, “Which Layer Height is Best for 3D Printing?,” 3dprinterly.com. Accessed: Jan. 28, 2022. [Online]. Available: https://3dprinterly.com/which-layer-height-is-best-for-3d-printing/

[28] F. Ross, “What is Layer Height in 3D Printing: The Ultimate Guide!,” https://ultimatelytech.com/what-is-layer-height-3d-printing/.

[29] N. Maguluri, G. Suresh, and K. V. Rao, “Assessing the effect of FDM processing parameters on mechanical properties of PLA parts using Taguchi method,” *Journal of Thermoplastic Composite Materials*, vol. 36, no. 4, pp. 1472–1488, Apr. 2023, doi: 10.1177/08927057211053036.

[30] H. Dou *et al.*, “Effect of Process Parameters on Tensile Mechanical Properties of 3D Printing Continuous Carbon Fiber-Reinforced PLA Composites,” *Materials*, vol. 13, no. 17, p. 3850, Aug. 2020, https://doi.org/10.3390/ma13173850

[31] D. L. Vinay, R. Keshavamurthy, and G. Ugrasen, “Tensile characteristics of metal filled 3D printed PLA based polymer composites,” *Interactions*, vol. 245, no. 1, p. 154, Jul. 2024,

https://doi.org/10.1007/s10751-024-01983-1

[32] M. Saleh, S. Anwar, A. Y. AlFaify, A. M. Al-Ahmari, and A. E. E. Abd Elgawad, “Development of PLA/recycled-desized carbon fiber composites for 3D printing: Thermal, mechanical, and morphological analyses,” *Journal of Materials Research and Technology*, vol. 29, pp. 2768–2780, Mar. 2024,

https://doi.org/10.1016/j.jmrt.2024.01.267